Journal of Molecular and Cellular Cardiology 47 (2009) 85–95

Contents lists available at ScienceDirect

Journal of Molecular and Cellular Cardiology

journal homepage: www.elsevier.com/locate/yjmcc

Original article

Rosiglitazone-induced heart remodelling is associated with enhanced turnover of myofibrillar protein and mTOR activation

William T. Festuccia [a,1], Mathieu Laplante [a,1], Sophie Brûlé [b], Vanessa P. Houde [b], Adel Achouba [c], Dominic Lachance [c], Maria L. Pedrosa [d], Marcelo E. Silva [d], Renata Guerra-Sá [d], Jacques Couet [c], Marie Arsenault [c], André Marette [b], Yves Deshaies [a,*]

[a] Department of Anatomy and Physiology, Faculty of Medicine and Laval Hospital Research Center, Laval University, Quebec, Canada G1V 4G5
[b] Department of Anatomy and Physiology, Faculty of Medicine and Lipid Research Unit, Laval University Hospital Research Center, Quebec, Canada G1V 4G2
[c] Department of Medicine, Faculty of Medicine and Laval Hospital Research Center, Laval University, Quebec, Canada G1V 4G5
[d] Department of Biological Sciences, ICEB, Federal University of Ouro Preto, MG, 35400-000, Brazil

ARTICLE INFO

Article history:
Received 13 October 2008
Received in revised form 8 April 2009
Accepted 17 April 2009
Available online 3 May 2009

Keywords:
Protein synthesis
Calpain/calpastatin
Proteasome
mTOR
AMPK
Peroxisome proliferator-activated receptor γ agonist
Glycogen
Rapamycin
MAPK

ABSTRACT

We investigated cardiac hypertrophy elicited by rosiglitazone treatment at the level of protein synthesis/degradation, mTOR, MAPK and AMPK signalling pathways, cardiac function and aspects of carbohydrate/lipid metabolism. Hearts of rats treated or not with rosiglitazone (15 mg/kg day) for 21 days were evaluated for gene expression, protein synthesis, proteasome and calpain activities, signalling pathways, and function by echocardiography. Rosiglitazone induced eccentric heart hypertrophy associated with increased expression of ANP, BNP, collagen I and III and fibronectin, reduced heart rate and increased stroke volume. Rosiglitazone robustly increased heart glycogen content (~400%), an effect associated with increases in glycogenin and UDPG-PPL mRNA levels and glucose uptake, and a reduction in glycogen phosphorylase expression and activity. Cardiac triglyceride content, lipoprotein lipase activity and mRNA levels of enzymes involved in fatty acid oxidation were also reduced by the agonist. Rosiglitazone-induced cardiac hypertrophy was associated with an increase in myofibrillar protein content and turnover (increased synthesis and an enhancement of calpain-mediated myofibrillar degradation). In contrast, 26S β5 chymotryptic proteasome activity and mRNA levels of 20S β2 and β5 and 19S RPN 2 proteasome subunits along with the ubiquitin ligases atrogin and CHIP were all reduced by rosiglitazone. These morphological and biochemical changes were associated with marked activation of the key growth-promoting mTOR signalling pathway, whose pharmacological inhibition with rapamycin completely blocked cardiac hypertrophy induced by rosiglitazone. The study demonstrates that both arms of protein balance are involved in rosiglitazone-induced cardiac hypertrophy, and establishes the mTOR pathway as a novel important mediator therein.

1. Introduction

Rosiglitazone and pioglitazone, two potent synthetic agonists of the peroxisome proliferator-activated receptor γ (PPARγ), are members of the thiazolidinedione (TZD) family of insulin-sensitizing compounds that are widely used in the treatment of insulin resistance and type 2 diabetes, two major risk factors for cardiovascular disease [1].

The overall outcome of the beneficial action of TZDs on insulin sensitization is confounded by untoward side effects such as weight (fat) gain, renal fluid retention with consequent edema and blood volume expansion, and perhaps cardiac dysfunction [2]. The impact of PPARγ activation on the heart has recently become of particular concern in the light of a meta-analysis of clinical reports suggesting increased risk for acute cardiac events in diabetic patients treated with rosiglitazone [2]. This issue adds up to existing concern related to possible deleterious effects of PPARγ activation on cardiac hypertrophy and heart failure in patients with pre-existing cardiac function impairment [3].

PPARγ is expressed at moderate levels in rodent hearts and its activation by TZDs has been contradictorily associated with either inhibition or stimulation of heart hypertrophy. More specifically, PPARγ agonists were demonstrated to inhibit cardiomyocyte hypertrophy induced in vitro by angiotensin II and mechanical stress [4,5]

* Corresponding author. Laval Hospital Research Centre, Institut – d'Youville Y3110, 2725 Chemin Sainte-Foy, Quebec, QC, Canada G1V 4G5. Tel.: +1 418 656 8711x3738; fax: +1 418 656 4942.
E-mail address: yves.deshaies@phs.ulaval.ca (Y. Deshaies).
[1] The two first authors contributed equally to the work reported in this manuscript.

0022-2828/$ – see front matter © 2009 Elsevier Inc. All rights reserved.
doi:10.1016/j.yjmcc.2009.04.011

and *in vivo* by aortic constriction [5], a model of pressure-induced cardiac enlargement. Supporting this putative inhibitory role of PPARγ towards heart hypertrophy, both heart-specific deletion and heterozygous mutation of PPARγ were demonstrated to, respectively, induce cardiac hypertrophy [6] and exacerbate the hypertrophic response to aortic constriction [5].

Paradoxically, several studies in rodent models have reported robust cardiac hypertrophy following relatively short-term treatment with PPARγ agonists, which has mainly been attributed to the increase in blood volume and consequent cardiac overload induced by these compounds [4,6–8]. The very recent findings, however, that cardiac PPARγ overexpression induces heart hypertrophy [9] characterized by increased left ventricular systolic dimension (dilated cardiomyopathy) suggest that PPARγ might have specific roles in the development of different types of heart remodelling.

Independently of the underlying cause, cardiac hypertrophy consists of the addition of new sarcomeres in parallel (concentric hypertrophy) or in series (eccentric hypertrophy) due to a positive balance between myofibrillar protein synthesis and degradation (proteolysis). Although several signalling pathways such as mitogen-activated protein kinases (MAPKs), among others, are involved in the development of cardiac hypertrophy, the mammalian target of rapamycin (mTOR) pathway, due to its role in promoting protein synthesis and regulating cell size, has recently emerged as a crucial regulator of heart remodelling. mTOR stimulates protein synthesis by activating p70 ribosomal S6 kinase (S6K) and by inhibiting eukaryotic translation initiating factor 4E (eIF4E) binding protein (4E-BP), a repressor of translation initiation [10]. mTOR has been implicated in several types of cardiac hypertrophy, including those induced by aortic constriction [11], thyroid hormones [12] and aerobic exercise [13].

In addition to synthesis, protein degradation mediated by the calpain/calpastatin and ubiquitin/proteasome systems, the major proteolysis pathways in the heart, has an important role in protein turnover and cardiac remodelling [14,15]. Whereas the calpain/calpastatin system comprises two calcium-dependent proteases and their endogenous allosteric inhibitor calpastatin, which are mainly localized in cardiac myofibrillar Z-discs [16], the proteasome system is a cytosolic multiplex of proteases that recognizes and hydrolyses poly-ubiquitinated proteins.

Considering the importance of protein turnover in heart remodelling and the relevance of TZDs to clinical practice, this study investigated the involvement of protein synthesis/degradation, mTOR, MAPK and AMP-activated protein kinase (AMPK) signalling pathways and associated changes in carbohydrate/lipid metabolism and heart function in cardiac hypertrophy elicited by chronic rosiglitazone administration. Finally, rosiglitazone treatment was combined with rapamycin, a potent mTOR inhibitor, to delineate the contribution of the mTOR signalling pathway in the cardiac hypertrophy induced by rosiglitazone.

2. Methods

2.1. Animals and treatments

Male Sprague–Dawley rats (200–225 g) (Charles River Laboratories, St. Constant, QC, Canada) were housed at 23 ± 1 °C with a 12:12 h light–dark cycle. Animal handling was in conformance with the Canadian Guide for the Care and Use of Laboratory Animals. All experimental procedures received prior approval of our animal care committee. Rats were fed a non-purified powdered rodent diet (Charles River Rodent Diet #5075, Woodstock, ON, Canada) alone (control) or supplemented with the PPARγ agonist rosiglitazone (AVANDIA) at a dose of 15 mg/kg day for 21 days. This dose of rosiglitazone was found in a preliminary dose–response study to be the lowest dose showing heart hypertrophy associated with redistribution of fat from visceral toward subcutaneous adipose depots, a hallmark of PPARγ agonist treatment in humans [17]. In a second protocol, control and rosiglitazone-treated rats were simultaneously treated for 15 days with daily injections of vehicle or rapamycin (2 mg/kg day, ip) in DMSO (1%) and suspended in carboxymethyl cellulose (0.2%). The dose of rapamycin was chosen based on previous studies showing its efficiency to completely block the mTOR pathway in rats and mice, such dose being within the rage of those used in human studies [18,19]. An extra group of rats was matched by weight and killed at day 0 of treatment to allow the estimation of heart weight gain by the various treatments. In both protocols, food intake was determined every other day by subtracting the amount of food remaining in the feeders from food initially provided. Unless otherwise specified, rats were killed in the fed state between 08:00 and 10:00 by anesthetic overdose and the heart was rapidly harvested and frozen in liquid nitrogen.

2.2. Serum determinations

Serum glucose concentration was measured by the glucose oxidase method. Serum insulin was determined by radioimmunoassay (Linco Research, St. Charles, MO). Serum triglycerides (Roche Diagnostics, Montreal, QC, Canada) and non-esterified fatty acids (NEFA C test kit, Wako, Richmond, VA) were measured enzymatically.

2.3. Plasma volume

Plasma volume was estimated in isoflurane-anesthetized rats by measuring Evans blue dilution after its intravenous injection as previously described [20].

2.4. Heart composition, lipoprotein lipase and glycogen phosphorylase activities

Heart DNA content was determined using a commercial kit (DNeasy tissue kit, Qiagen, Mississauga, ON, Canada). Cardiac glycogen content was measured exactly as previously described [21]. Heart triglyceride content was determined enzymatically (Trig/GB, Roche Diagnostics, Montreal, QC, Canada) in total lipid extracts prepared as previously described [22]. Heart lipoprotein lipase (LPL) activity was measured by incubating 100 μl of heart homogenates for 1 h at 28 °C with 100 μl of a substrate mixture consisting of 0.2 mol/l Tris–HCl buffer, pH 8.6, which contained 10 MBq/l [*carboxyl*-^{14}C]triolein (Amersham, Oakville, ON, Canada) and 2.52 mmol/l cold triolein emulsified in 50 g/l gum arabic, as well as 20 g/l fatty acid-free bovine serum albumin, 10% porcine serum as a source of apolipoprotein C-II, and either 0.2 or 2 M NaCl. Free oleate released by LPL was then separated from intact triolein, and sample ^{14}C radioactivity was determined in a scintillation counter. LPL activity was calculated by subtracting lipolytic activity determined in a final NaCl concentration of 1 M (non-LPL activity) from total lipolytic activity measured in a final NaCl concentration of 0.1 M. LPL activity was expressed as microunits (1 μU = 1 μmol NEFA released per hour of incubation at 28 °C). Heart glycogen phosphorylase (PyGM) activity was measured as previously described [23]. Briefly, hearts were homogenized in ice-cold buffer (100 mM Na_2HPO_4, 100 mM KH_2PO_4, 2 mM EDTA and 1 mM PMSF), centrifuged and the supernatant was collected and used for enzyme assay. PyGM activity was estimated by the reduction of NADP to NADPH in a spectrophotometer at 25 °C with wavelength of 340 nm for 15 min. The reaction medium was composed of 50 mM triethanolamine, 10 mM Na_2HPO_4-KH_2PO_4, 5 mM EDTA, 10 mM $MgCl_2$, 10 mM L-cysteine, 2 mM AMP, 0.3 mM NADP, 0.05 mM glucose 1-6 diphosphate, 1 U/sample glucose 6-phosphate dehydrogenase (G6PDH), 5 U/sample phosphoglucomutase and 0.4 mg/sample glycogen.

2.5. Heart glucose uptake

The rate of glucose uptake by the heart was estimated *in vivo* essentially as previously described [24,25]. Briefly, 0.2 ml of a 2-deoxy-1-^{3}H-glucose (30 μCi, New England Nuclear, 11 Ci/mmol) in 0.9% NaCl solution was injected though a catheter inserted in the jugular vein and 0.2 ml of blood was collected at 1, 3, 5, 10, 20, 40 and 60 min after label injection for radioactivity and glucose estimation. Upon collection, blood was immediately deproteinized in $Ba(OH)_2/ZnSO_4$ as previously described [26] and centrifuged (2 min, 16,000 ×*g*). The supernatant was used for the determination of blood glucose with a glucose oxidase kit (Wako Chemicals, Richmond, VA) and 2-deoxy-1-^{3}H-glucose in a liquid-scintillation counter (Tri-Carb 2900TR, PerkinElmer, IL). After 60 min, rats were killed by overdose of ketamine/xylazine and tissues were used for determining the content of 2-deoxy-[1-^{3}H]glucose 6-phosphate. Rates of glucose uptake were calculated as previously described [25]. Blood glucose levels did not significantly change during the sampling period in either group, a requirement of the technique used.

2.6. Glycogen staining

Sections from paraffin-embedded mid-left ventricles were stained using periodic acid-Schiff (PAS) following supplier's protocol (Sigma Markham, Ontario, CA). Briefly, sections were de-paraffinized, hydrated and immersed in periodic acid solution. The slides were then rinsed and immerged in Schiff's reagent for 15 min at 25 °C. Negative control slides were treated with α-amylase before glycogen staining.

2.7. RNA extraction and analysis

Heart total RNA isolation, reverse transcription and quantification by real-time polymerase chain reaction (PCR) were carried out as previously described [27]. Primers used for the PCR reactions are described in Electronic Supplemental Table S1. Data are expressed as the ratio between the expression of the target gene and the housekeeping gene 36B4, the expression of which is not significantly affected by rosiglitazone or rapamycin treatment.

2.8. In vivo protein synthesis

Rates of heart protein synthesis were measured *in vivo* with a flooding dose of ^{3}H-phenylalanine (15–30 Ci/mmol, 150 mM, 1 ml/100 g body weight) injected into the jugular vein essentially as previously described [28,29]. Hearts were processed for analysis of phenylalanine incorporated into different protein fractions exactly as previously described [29]. Briefly, whole hearts were homogenized in ice-cold water (200 mg/ml) and portions of 1 ml were either immediately precipitated with perchloric acid or destined for protein fractionation (see below). The acid supernatant was used for determination of free phenylalanine, whereas the pellet was subjected to alkali digestion before protein measurement by the bicinchoninic acid method (BCA protein assay kit, Rockford, IL, USA). Proteins were then re-precipitated, hydrolyzed and incubated with tyrosine decarboxylase to obtain the specific radioactivity of phenylalanine in the various protein fractions.

Heart proteins were fractionated by mixing with a low ionic buffer (10 mM imidazole, 60 mM KCl, 0.5 mM EGTA, 4 mM $MgCl_2$, 1 mM sodium azide, 1 mM dithiothreitol, and 0.5% (v/v) Triton X-100, pH 7.0) and centrifuged at 2000 ×*g* for 15 min at 4 °C. The supernatant (sarcoplasmic fraction) was decanted and the pellet was disrupted in a high ionic strength buffer (100 mM K phosphate monobasic, 50 mM K phosphate dibasic, 300 mM KCl, 1 mM EDTA and 5 mM ATP, pH 6.3) and centrifuged. The supernatant (myofibrillar fraction) was decanted and the remaining pellet constituted the stromal fraction. All three fractions were processed as described above.

2.9. 26S β5 (chymotryptic) proteasome activity

Heart 26S β5 (chymotryptic) proteasome activity was measured as previously described [30–32]. Briefly, heart samples were homogenized using a Polytron homogenizer in buffer A (20 mM Tris, 20 mM KCl, 10 mM Mg acetate, 2 mM DTT, 10% glycerol, pH 7.6). The soluble protein fraction was isolated by centrifugation at 30,000 ×*g* for 30 min at 4 °C. The pellet was discarded and the supernatant fraction was centrifuged again at 100,000 ×*g* for 6 h. The supernatant fraction was discarded and the pellet was carefully washed in fresh buffer A, which was also discarded. The washed pellets were re-suspended in 1 ml of buffer A. Proteasome activity was measured by the release of 7-amino-4-methylcoumarin from Suc-LLVY-7-amido-4 methylcoumarin (Sigma-Aldrich, Poole, UK). Aliquots of each sample were incubated with an equal volume of reaction mixture containing 100 mM Tris (pH 7.5), 20 mM $MgCl_2$, 0.5 mM DTT, and 0.1 mM peptide substrate. In the presence of $MgCl_2$, the proteasome has enough ATP to show proteolytic activity [33]. The reaction was allowed to proceed for 30 min at 37 °C and stopped by the addition of 1 ml 0.1 M Na borate and 80 μl of 20% (w/v) SDS. The product was measured at an emission wavelength of 440 nm (λ excitation = 380 nm) using slit widths for excitation = 5 nm, and emission = 10 nm.

2.10. Calpain activity

Heart calpain activity was measured with a kit from BioVision (BioVision Research Products, CA). Briefly, hearts were homogenized in the extraction buffer provided in the kit and centrifuged at 10,000 ×*g*, 4 °C for 5 min. The supernatant was collected and destined for protein measurement with bicinchoninic acid method. Calpain activity assay was performed in quadruplicates with 200 μg of heart protein in the presence or absence of calpain inhibitor Z-LLY-FMK (BioVision, final concentration 50 μM). Reaction was carried out at 37 °C in the dark for 1 h and fluorescence was read in a microplate fluorescence reader (BioTek Instruments, Winooski, VT) with 400 nm excitation and 505 nm emission. Active human calpain (BioVision) was used as a positive control. Calpain activity was calculated by the difference of relative fluorescence units (RFU) of samples in the presence and absence of calpain inhibitor.

In addition to the proteolytic enzymes described above, the activity of lysosomal cathepsins D and L was quantified as described in the Electronic Supplemental Material.

2.11 Protein quantification by Western blot

Because the signal transduction pathways investigated in the present study are profoundly affected by the nutritional status, in an attempt to standardize metabolic conditions and reduce inter-individual variability, control and rosiglitazone-treated rats were killed after a 12-h fast followed by 3 h of refeeding. Frozen hearts were homogenized in lysis buffer (50 mM HEPES, pH 7.5, 150 mM NaCl, 1 mM EGTA, 20 mM β-glycerophosphate, 1% NP-40, 10 mM NaF, 2 mM Na_3VO_4 and a cocktail of protease inhibitors), subjected to sodium dodecyl sulfate (SDS)-polyacrylamide gel electrophoresis, transferred to nitrocellulose membranes, blocked for 1 h and incubated overnight at 4 °C with primary antibodies. After washing, membranes were incubated with immunoglobulin G conjugated to horseradish peroxidase, washed again and the immunoreactive bands were detected by the enhanced chemiluminescence method. Densitometric analysis was performed with ImageQuant TL software (GE Healthcare, Little Chalfont, UK). Antibodies used in the

Table 1
Morphometric variables, serum metabolites and hormones, plasma volume and hematocrit in control and rosiglitazone-treated rats.

	Control	Rosiglitazone
Initial weight (g)	256.1 ± 1.9	256.9 ± 2.1
Final weight (g)	413.6 ± 7.1	425.1 ± 10.0
Weight gain (g)	157.5 ± 6.1	168.2 ± 10.5
Food intake (g)	654.8 ± 17.9	699.8 ± 16.3
Food efficiency (g/MJ)	18.6 ± 0.3	18.7 ± 1.1
Glucose (mmol/l)	8.3 ± 0.1	7.7 ± 0.2*
Triglycerides (mmol/l)	1.8 ± 0.2	0.7 ± 0.1*
NEFA (mmol/l)	0.50 ± 0.05	0.22 ± 0.01*
Insulin (pmol/l)	419 ± 58	218 ± 18*
Adiponectin (μg/ml)	10 ± 1.6	38 ± 6.0*
Plasma volume (ml/100 g bw)	5.33 ± 0.17	6.28 ± 0.23*
Hematocrit (%)	46 ± 0.36	40 ± 0.39*

Morphometric and food intake values are means ± SEM of 10–12 rats. Fasting serum values are means ± SEM of 6 rats. Insulin was measured in the postprandial state. Bw: body weight.
* $P<0.05$ versus control.

Western blots are described in the Electronic Supplemental Material.

2.12. Echocardiography

Echocardiographic analysis was performed using a 12 MHz phased-array transducer coupled to a Sonos 5500 echocardiography ultrasound (Philips Medical Imaging, Andover, MA) as previously described [34]. Stroke volume was calculated by pulsed Doppler in the left ventricular outflow tract. Ejection fraction was calculated as previously described [35]. Diastolic filling pattern was evaluated from the *E* wave to *A* wave (*E*/*A*) ratio of the mitral pulsed Doppler flow at the tip of mitral leaflets. Relative wall thickness was calculated as the ratio of the sum of diastolic septal and posterior wall thicknesses to left ventricular end-diastolic diameter. Left ventricular (LV) mass was calculated with the following formula:

$$\text{LV mass} = 1.04 \times (\text{EDD} + \text{PW} + \text{SW})^3 - \text{EDD}^3$$

where EDD is the end-diastolic diameter, PW is the posterior wall thickness and SW is the septal wall thickness. LV ejection time (ET) was measured from the beginning to end of the aortic flow wave. Mitral flow was recorded at the tip of the mitral valve from an apical view using Doppler. Maximal velocity and velocity-time integral (VTI) of the *E* wave were measured and the isovolumic relaxation time (IVRT) was measured as the interval between aortic closure and the start of mitral flow. The myocardial performance index (MPI), which is inversely related to combined systolic and diastolic myocardial performance, was calculated as previously described [36]. Early lateral mitral annulus movement (E_a) was recorded as previously described [37]. The *E* wave-to-E_a ratio (E/E_a) is reported as an index of filling pressures.

2.13. Norepinephrine turnover

Heart norepinephrine (NE) turnover rates (NETO) were estimated from the decline in tissue NE content after inhibition of catecholamine synthesis with DL-α-methyl-tyrosine ester (α-MT; Sigma, St. Louis, MO) as previously described [27]. Rates of NETO were calculated as the product of the fractional turnover rate (k) and the endogenous NE content at time 0 as previously described [38]. Fractional turnover rate (k) was calculated by the formula:

$$k = (\log [\text{NE}]_0 - \log [\text{NE}]_4) / (0.434 \times 4)$$

where $[\text{NE}]_0$ and $[\text{NE}]_4$ are the NE content at times 0 and 4 h, respectively.

2.14. Statistical analysis

Results are expressed as means ± SEM. Simple effects of rosiglitazone treatment were analyzed by Student's unpaired *t* test. When appropriate, factorial ANOVA followed by Newman–Keuls' multiple range test was used for multiple comparisons. $P<0.05$ was taken as the threshold of significance.

3. Results

Final body weight, body weight gain, food intake and efficiency were not significantly affected by rosiglitazone treatment (Table 1). Confirming its beneficial effects on insulin sensitivity and lipemia, rosiglitazone significantly reduced fasting serum glucose (−7%), insulin (−48%), triglyceride (−61%), and non-esterified fatty acid (−60%) levels. Also as expected, rosiglitazone significantly increased adiponectin levels (4-fold) and plasma volume (+18%), and reduced hematocrit (−13%).

As summarized in Table 2, rosiglitazone markedly increased heart weight expressed as either absolute (+30%) or relative to both body weight (+23%) or tibia length (+33%), indicating that rosiglitazone-induced heart remodelling was not related to changes in overall body growth. The rosiglitazone-induced increase in heart weight was due to a similar growth of all heart chambers as evidenced by the increased weight of left and right ventricles (+25%), and right (+57%) and left (+42%) atria that were confirmed by echocardiography (Electronic Supplemental Table S2). Rosiglitazone-induced heart remodelling was associated with a significant increase in cardiac DNA content per unit of tissue weight (+55%), and mRNA levels of atrial natriuretic peptide 1 (ANP, +142%, Table 2) and type B natriuretic peptide (BNP, +106%, Table 2), two markers of heart hypertrophy. Furthermore, collagen I and III and fibronectin mRNA levels were significantly higher in rosiglitazone-treated rats compared to controls (Table 2). No notable change, however, was observed in the overall ventricular amount of fibrosis in rosiglitazone-treated rats (not shown). Moreover, such morphological changes did not affect left ventricular ejection fraction as evaluated by echocardiography (Table 3). Rosiglitazone treatment significantly decreased heart rate (−10%) and tended ($P=0.1$) to increase stroke volume (+10%), such that no change in cardiac output ensued. Rosiglitazone increased the E/A (+33%) and E/E_a (+18%) ratios, and the MPI, a composite negative index of general myocardial performance, tended to be increased ($P=0.07$) in rosiglitazone-treated rats. These functional changes were associated with reduced heart sympathetic activity as evidenced by reduced cardiac NE levels and NETO of rosiglitazone-treated rats compared to controls.

Table 2
Heart chamber weight, DNA content and cardiac mRNA levels of atrial natriuretic and B-type natriuretic peptides (ANP and BNP, respectively) and extracellular matrix components in control and rosiglitazone-treated rats.

	Control	Rosiglitazone
Heart weight, g	1.06 ± 0.03	1.37 ± 0.03*
Heart (% bw)	0.26 ± 0.01	0.32 ± 0.01*
Heart weight/tibia length (mg/mm)	18.2 ± 0.6	24.0 ± 0.5*
LV + RV weight, g	0.98 ± 0.035	1.22 ± 0.027*
RA weight, mg	29.6 ± 3.2	46.7 ± 5.6*
LA weight, mg	31.9 ± 4.1	45.5 ± 5.1*
DNA (μg/g heart)	138 ± 10	215 ± 34*
ANP/36B4 mRNA	1.0 ± 0.17	2.43 ± 0.4*
BNP/36B4 mRNA	1.0 ± 0.08	2.7 ± 0.13*
Fibronectin mRNA	1.0 ± 0.1	1.7 ± 0.1*
Collagen I mRNA	1.0 ± 0.07	1.73 ± 0.27*
Collagen III mRNA	1.0 ± 0.15	1.84 ± 0.31*

LV: left ventricle; RV: right ventricle; RA: right atrium; LA: left atrium; bw: body weight. Values are means ± SEM of 10 rats.
* $P<0.05$ versus control.

Table 3
Cardiac mechanical, diastolic, hemodynamic and sympathetic activities in control and rosiglitazone-treated rats.

	Control	Rosiglitazone
Ejection fraction (%)	74.9 ± 1	74.5 ± 1
E wave	94.4 ± 3.04	111.8 ± 2.81*
A wave	80.1 ± 6.07	70.2 ± 3.18
E/*A* ratio	1.22 ± 0.070	1.63 ± 0.110*
Slope E	2609 ± 105.5	2430 ± 108.2
E/E_a	13.0 ± 0.62	15.3 ± 0.66*
MPI	0.36 ± 0.027	0.43 ± 0.022
LA diameter, mm	4.3 ± 0.09	4.9 ± 0.14*
Heart rate, bpm	369 ± 6.7	333 ± 5.8*
Stroke volume, μl	220 ± 6.1	242 ± 11.0
Cardiac output, ml	81.3 ± 2.48	80.6 ± 3.26
NE content (ng/tissue)	1050 ± 23	928 ± 37*
k (%/h)	9.3 ± 0.7	8.1 ± 0.4
NETO (ng NE/tissue h)	99 ± 9.2	75.2 ± 7*

E wave: *E* wave maximal velocity by pulsed Doppler of mitral flow; *A* wave: *A* wave maximal velocity by pulsed Doppler of mitral flow. E_a: Peak velocity of the mitral valve annulus during early diastolic expansion. MPI: myocardial performance index (or Tei) index. NE: norepinephrine. *k*: NE fractional turnover rate. NETO: NE turnover. Values are means ± SEM of 10 rats.
* $P<0.05$ versus control.

As depicted in Fig. 1, rosiglitazone markedly enhanced heart glycogen deposition as evidenced by the increase in glycogen content per g of tissue (+344%, Fig. 1A) and histological glycogen labelling of heart sections (Fig. 1B). Glycogen accumulation was associated with an increase in cardiac mRNA levels of proteins involved in glycogen synthesis glycogenin (+90%) and UDP-linked glucose pyrophosphorylase (UDPG-PPL, +40%) without affecting those of glycogen synthase (GyS1) (Fig. 1C). Regarding glycogenolysis, rosiglitazone significantly decreased glycogen phosphorylase (PyGM) mRNA levels and activity (−16 and −27%, respectively, Figs. 1C and D). No change was seen in the content of either phosphorylated glycogen synthase (GS) or glycogen synthase kinase 3 α/β (GSK3), a covalent regulator of GS activity (Figs. 1E and F). Because constitutive activation of the AMPK pathway in the heart is associated with increased cardiac glycogen stores [39], we next evaluated the effects of rosiglitazone treatment on components of this signalling pathway. Cardiac AMPK was positively affected by rosiglitazone as revealed by increased phosphorylation of AMPK (Thr172) and of its downstream target acetyl CoA carboxylase (ACC, Ser79) (Fig. 2F).

In contrast to glycogen deposition, PPARγ agonist-induced heart remodelling was associated with a significant reduction in cardiac TG content (−18%, Fig. 2A) along with a decrease in the activity and mRNA levels of LPL (−45% and 18%, respectively, Figs. 2B and D). With regard to proteins involved in fatty acid uptake and transport, rosiglitazone significantly increased mRNA levels of FAT/CD36 (+40%) without affecting those of the fatty acid transporter protein 1 (FATP1) and fatty acid binding protein 3 (FABP3) (Fig. 2D). In association with heart TG levels, rosiglitazone significantly reduced mRNA levels of acetyl-coenzyme A dehydrogenase medium chain (ACADM, −42%) and very long chain (ACADVL, −31%), proteins involved in fatty acid oxidation, without affecting those of carnitine palmitoyltransferase 1 (CPT1), acetyl-coenzyme A dehydrogenase long chain (ACADL), or pyruvate dehydrogenase kinase 2 (PDK2) (Fig. 2E). A trend towards a decrease in peroxisome proliferator-activated receptor α (PPARα) mRNA levels was observed (−28%, $P=0.06$, Fig. 2E). Regarding carbohydrate metabolism, rosiglitazone markedly increased cardiac glucose uptake (+65%, Fig. 2C) and mRNA levels of glucose 6-phosphate dehydrogenase (G6PDH, +33%, Fig. 2F). In contrast, lactate dehydrogenase (LDH) mRNA levels were significantly decreased (−20%, Fig. 2F) by rosiglitazone.

Rosiglitazone-induced heart remodelling was associated with changes in cardiac protein metabolism as evidenced by the increase in total heart content of myofibrillar (+38%), sarcoplasmic (+36%), and stromal (+26%) protein fractions (Table 4). Synthesis of

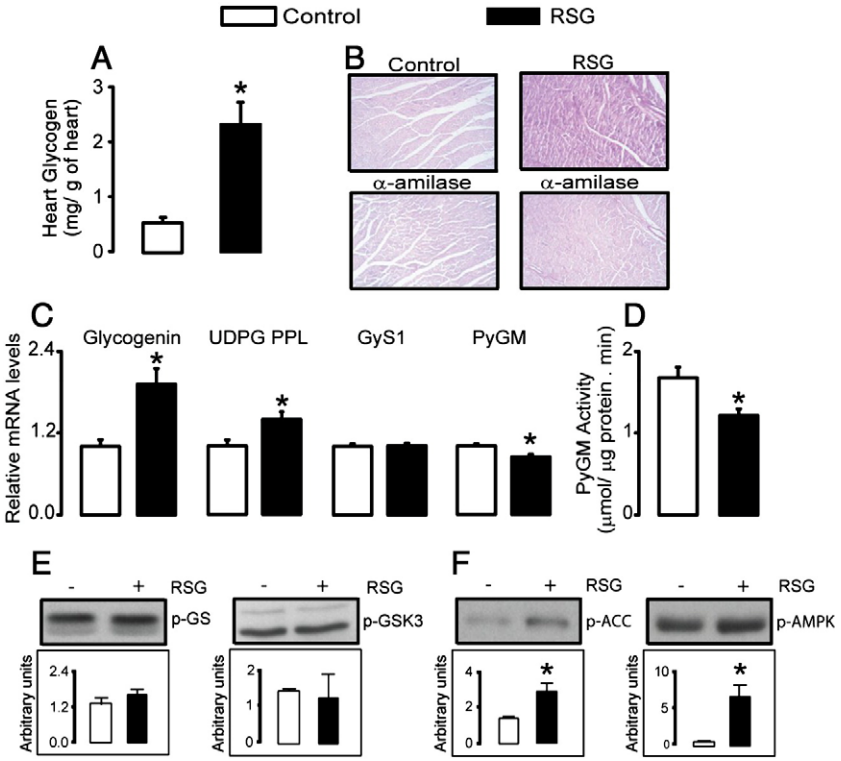

Fig. 1. Heart glycogen content (panels A and B), mRNA levels of glycogenin, UDPG-pyrophosphorylase (PPL), glycogen synthase 1 (GyS1) and glycogen phosphorylase (PyGM) (panel C), PyGM activity (panel D), protein content of phospho-glycogen synthase Ser645/649/653/657 (p-GS) and phospho-glycogen synthase kinase-3α/β Ser21/9 (p-GSK3) (panel E), and of phospho-acetyl-CoA carboxylase Ser79 (pACC) and phospho-AMPKα Thr172 (p-AMPK) (panel F) in rats treated or not with rosiglitazone (RSG, 15 mg/kg day) for 21 days. $n=6$–8 rats per group. *$P<0.05$ versus control.

myofibrillar protein was significantly increased by rosiglitazone as evidenced by the higher rates of protein synthesis expressed both per unit RNA (+34%) and as absolute rate (+69%). In addition, rosiglitazone tended to increase the percentage of myofibrillar protein renewed each day (fractional rate, +24%, $P=0.07$). No significant change was seen in the rate of sarcoplasmic or stromal protein synthesis expressed either as fractional or as relative to RNA, whereas stromal absolute rate was significantly increased (+34%) by rosiglitazone.

Regarding proteolysis, rosiglitazone markedly increased heart calpain activity (+63%) and reduced mRNA levels and protein content of calpastatin (−33% and −25%, respectively), an endogenous allosteric inhibitor of calpains 1 and 2, whose mRNA levels were not altered by rosiglitazone (Figs. 3A–C). With respect to the lysosomal proteolytic pathway, rosiglitazone did not significantly affect activities and mRNA levels of cathepsin D and L (Electronic Supplemental Fig. S1). In contrast to calpain and lysosomal proteolysis, rosiglitazone markedly decreased 26S β5 (chymotryptic) proteasome activity (−57%, Fig. 3) and mRNA levels of 20S β2 (−20%) and β5 (−60%) and 19S regulatory particle non-ATPase (RPN) 2 (−35%) proteasome subunits (Figs. 3D and E). Protein content of β5 was also reduced by rosiglitazone (−31%, Fig. 3H). In addition, rosiglitazone reduced mRNA levels of the ubiquitin ligases atrogin-1 (−26%) and carboxy terminus of Hsp70 interacting protein (CHIP, −16%) (Fig. 3F). The mRNA levels of genes coding for the 20S α1 and α7 and 19S regulatory particle triple A (RPT) 1 proteasome subunits and the ubiquitin ligases muscle-specific RING finger protein 1 (MuRF1) and E3-αII, along with the protein contents of α7 and RPT 1, were not affected by rosiglitazone (Figs. 3E–G and I).

Concerning signalling pathways that target protein metabolism, rosiglitazone significantly increased heart content of phosphorylated

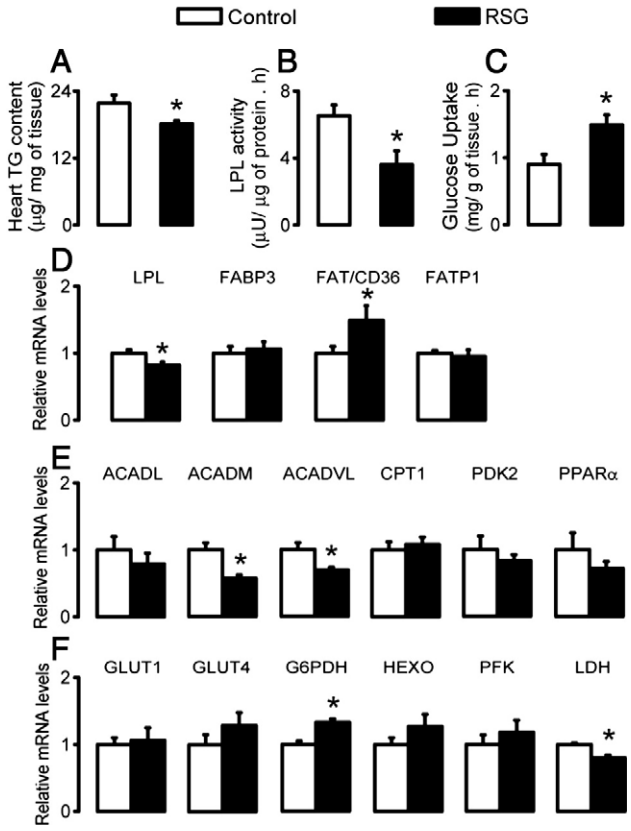

Fig. 2. Heart triglyceride (TG) content (panel A), lipoprotein lipase (LPL) activity (panel B), *in vivo* glucose uptake (panel C), and mRNA levels of proteins involved in fatty acid uptake and transport (panel D), in fatty acid oxidation (panel E), and glucose transport and metabolism (panel F) in rats treated or not with rosiglitazone (RSG, 15 mg/kg day) for 21 days. $n=8$–12 rats per group. *$P<0.05$ versus control.

Table 4
Heart sarcoplasmic, myofibrillar and stromal protein content and *in vivo* rates of synthesis in control and rosiglitazone-treated rats.

	Control	Rosiglitazone
Myofibrillar protein (mg/heart)	168 + 6	223 + 13*
Fractional synthesis (k_s, %/day)	11.5 ± 1.5	14.3 ± 0.6
Synthesis per unit RNA (k_{RNA}), mg prot/(day mg RNA)	12.3 ± 1.5	16.5 ± 0.9*
Absolute synthesis (V_s, mg prot/day)	19.4 ± 2.4	31.9 ± 1.7*
Sarcoplasmic protein (mg/heart)	237 + 3	323 + 27*
Fractional synthesis (k_s, %/day)	15.7 ± 2	18.5 ± 1.9
Synthesis per unit RNA (k_{RNA}), mg prot/(day mg RNA)	23.6 ± 3.1	30.6 ± 3.1
Absolute synthesis (V_s, mg prot/day)	37.4 ± 5.2	59.8 ± 8.8
Stromal protein (mg/heart)	89.8 + 4.8	114 + 3.5*
Fractional synthesis (k_s, %/day)	12.3 ± 0.9	12.9 ± 0.4
Synthesis per unit RNA (k_{RNA}), mg prot/(day mg RNA)	6.9 ± 0.6	7.6 ± 0.2
Absolute synthesis (V_s, mg prot/day)	11.0 ± 0.7	14.8 ± 1.3*

Values are means ± SEM of 6 rats.
* $P<0.05$ versus control.

mTOR (Ser2448) relative to controls (Fig. 4A). Activation of the mTOR pathway by rosiglitazone was confirmed at the level of downstream mTOR substrates, as evidenced by the significant increase in phosphorylated S6K1, S6, and 4E-BP1 contents (Figs. 4B–D). eEF2 phosphorylation (Thr56), however, was increased by rosiglitazone (Fig. 4E). The level of phosphorylated Akt (Ser473) was not significantly affected by rosiglitazone (Fig. 4A). Confirming a previous study [6], rosiglitazone markedly increased phosphorylated cardiac active contents of P38 MAPK, extracellular signal-related kinase (ERK), and c-Jun N-terminal kinase (JNK) (Electronic Supplemental Figs. S2A–C).

In an attempt to determine the contribution of mTOR signalling to the cardiac remodelling induced by rosiglitazone, rats were concomitantly treated for 15 days with rosiglitazone and rapamycin, a potent mTOR inhibitor. As depicted in Fig. 5, rapamycin completely blocked activation of the mTOR pathway induced by rosiglitazone, as evidenced by the abolition of the rosiglitazone-induced increase in cardiac phosphorylated contents of S6K1 and S6 (Figs. 5A and B). In addition to the mTOR pathway, rapamycin blocked the increase in phosphorylated ERK induced by rosiglitazone, without affecting JNK or AMPK phosphorylation (Figs. 5C, E and F). In contrast, rapamycin further increased phosphorylated P38 in rosiglitazone-treated rats (Fig. 5D). In association with these signalling pathways, rapamycin treatment completely blocked the increase in cardiac final weight, weight gain and ANP mRNA levels induced by rosiglitazone (Figs. 5G–I). Furthermore, rapamycin treatment did not affect the decrease in hematocrit and only partially blocked the increase in BNP mRNA levels and plasma adiponectin induced by rosiglitazone (Figs. 5J, L and M).

4. Discussion

The aim of the present study was to characterize rosiglitazone-induced heart remodelling in an attempt to improve our understanding of its underlying mechanisms and consequences on heart function. Chronic rosiglitazone induced eccentric heart hypertrophy that was associated with increased expression of ANP and BNP and changes in heart function, including reduced heart rate and increased stroke volume. Rosiglitazone also robustly increased heart glycogen content, glycogenin and UDPG-PPL mRNA levels and reduced PyGM expression and activity. In association, activity of AMPK signalling was also increased by the agonist. Rosiglitazone-induced hypertrophy was associated with increased turnover of myofibrillar proteins due to increased synthesis and an enhancement of calpain-mediated myofibrillar degradation. Protein degradation through the ubiquitin–proteasome appeared, however, to be reduced by rosiglitazone. These morphological and biochemical changes were associated with marked activation of the key growth-promoting signalling pathways MAPK

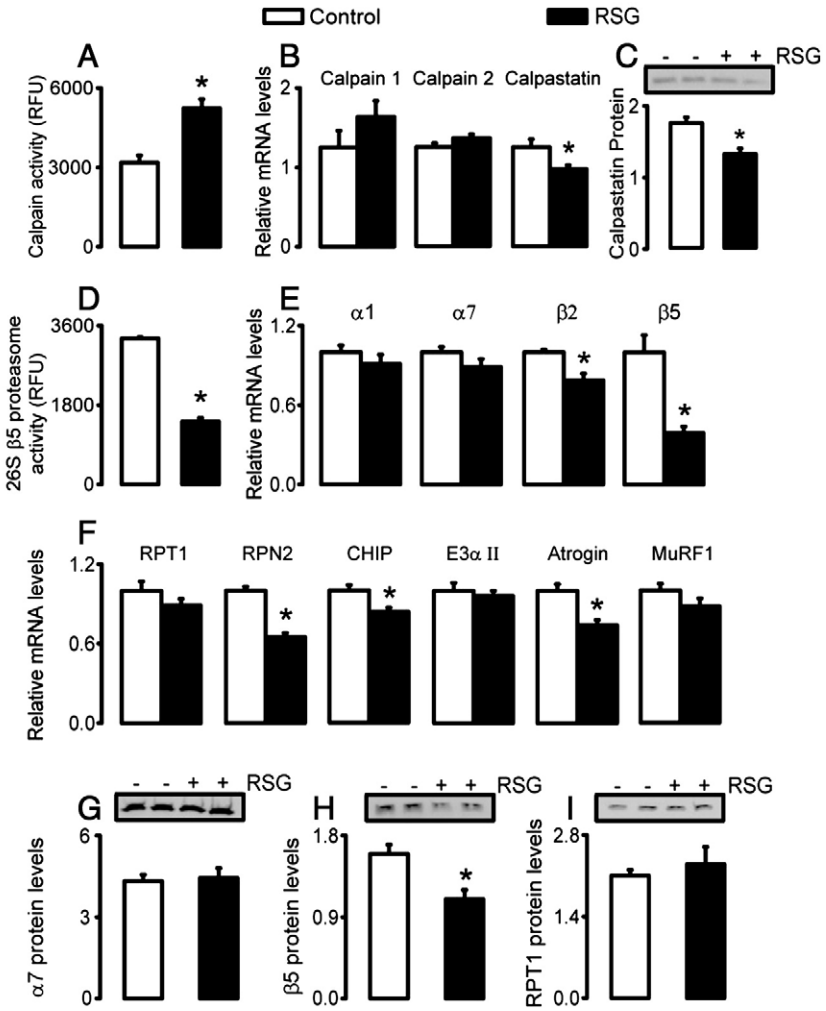

Fig. 3. Heart activities of calpain (panel A) and 26S β5 chymotryptic proteasome (panel D), mRNA levels of calpains–calpastatin (panel B), 20S and 19S proteasome subunits (panels E and F, respectively) and ubiquitin ligases (panel F), and protein content of calpastatin and α7, β5 and RPT1 proteasome subunits (panels C, G, H and I, respectively) in rats treated or not with rosiglitazone (RSG, 15 mg/kg day) for 21 days. $n = 6$–8 rats per group. *$P<0.05$ versus control.

and especially mTOR, whose pharmacological inhibition with rapamycin resulted in a complete abolition of cardiac hypertrophy induced by rosiglitazone.

Confirming previous studies [6–8], chronic rosiglitazone treatment was associated with a marked enlargement of all cardiac chambers. Hypertrophy, characterized as eccentric due to increased diastolic and systolic diameter and reduced relative wall thickness, was associated with a marked increase in tissue DNA content, probably due to multinucleation [40], and cardiac levels of ANP and BNP, two markers of heart hypertrophy. Some remodelling of the extracellular matrix also appeared to occur as evidenced by the abnormally high mRNA levels of collagen I and III and fibronectin. Functional heart analysis revealed that rosiglitazone administration resulted in reduced heart rate associated with lower cardiac sympathetic activity, slightly higher stroke volume, and normal cardiac output. Furthermore, echocardiography was suggestive of slightly abnormal diastolic filling. Whether this might be translated into increased myocardial fibrosis and left ventricular dysfunction after longer exposure to rosiglitazone is unknown but clearly deserves further investigation.

In line with several pathological conditions leading to hypertrophic cardiomyopathy [39,41], rosiglitazone-induced heart remodelling was associated with a marked increase in cardiac glycogen content and mRNA levels of its protein primer glycogenin and of UDPG-PPL, an enzyme that generates UDP-linked glucose for glycogen synthesis. The absence of change in the phosphorylated content and mRNA levels of GS and its major regulator GSK-3, however, excludes covalent modification of this enzyme as a possible mechanism for this effect. Instead, given that PPARγ agonism increases *in vivo* heart uptake and utilization of glucose, as shown here and previously [7,42], rosiglitazone-induced glycogen accumulation might be due to a combination of allosteric activation of GS by high intracellular levels of glucose 6-phosphate and lesser recruitment of its intracellular stores, as supported by reduced mRNA levels and activity of the glycogenolytic enzyme PyGM observed here. Interestingly, rosiglitazone-induced glycogen accumulation was associated with increased activity of the AMPK signalling pathway, whose long-term pharmacologic [43] and genetic [39] activation has been associated with increased glucose uptake and glycogen storage by skeletal muscle and the heart, respectively. These data suggest a possible involvement of AMPK, likely activated by adiponectin, whose plasma levels are robustly increased by rosiglitazone, as a possible mediator of cardiac glycogen accumulation induced by PPARγ agonism.

In the normal heart, most of the ATP (approximately 60%) comes from the oxidation of fatty acids taken up from the circulation, mainly triglycerides. Previous studies have shown that PPARγ agonism brings about a shift from fatty acid towards glucose utilization in the rat heart [7,42]. Congruent with these findings, rosiglitazone treatment was associated with a marked increase in heart glucose uptake and a reduction in LPL activity which provides fatty acids to the tissue by mediating lipolysis of circulating VLDL and chylomicron-TG. This was

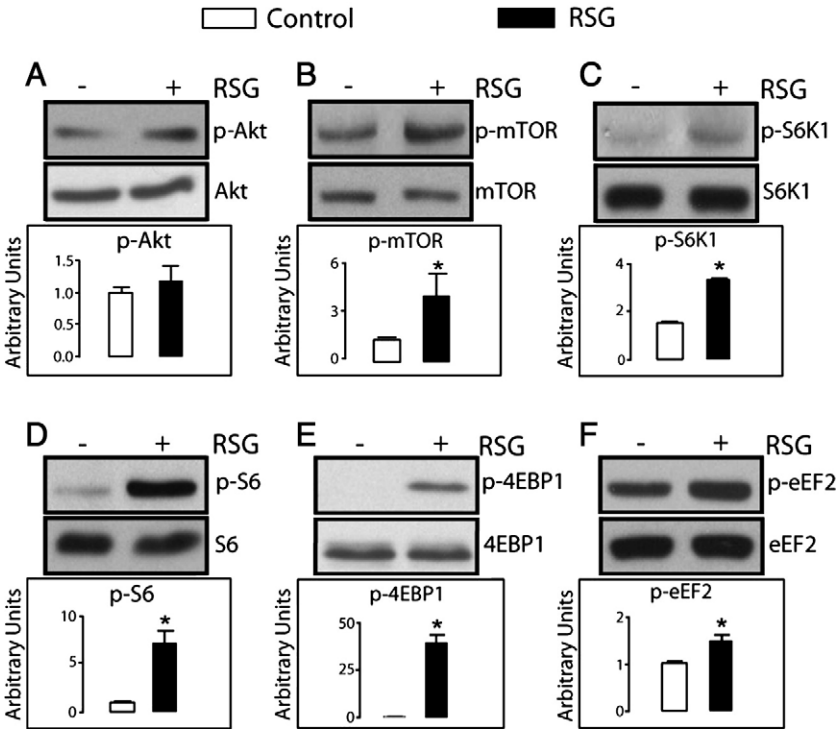

Fig. 4. Heart content of phospho-Akt Ser473 (p-Akt, panel A), phospho-mTOR Ser2448 (p-mTOR, panel B), phospho-p70 S6 Kinase Thr389 (p-S6K1, panel C), phoS6 Ribosomal Protein Ser240/244 (p-S6, panel D), 4E-BP1 Ser65 (p-4EBP1, panel E), eEF2 Thr56 (p-eEF2 panel F) and their respective total protein content in rats treated or not with rosiglitazone (RSG, 15 mg/kg day) for 21 days. $n = 4$–6 rats per group. *$P < 0.05$ versus control.

followed by a reduction in the expression of fatty acid oxidation genes and a trend toward an increase in those of glucose metabolism. In addition, mRNA levels of LDH, which converts pyruvate to lactate through anaerobic glycolysis, were reduced by rosiglitazone, suggesting a reinforcement of glucose flux toward oxidation via the Krebs cycle. Such a switch from fatty acids to glucose as the major source of energy substrate is frequently associated with the development of pathological cardiomyopathy [44], and may be considered as a potential deleterious effect of rosiglitazone on cardiac metabolism.

Concerning protein metabolism, rosiglitazone-induced hypertrophy was associated with an increase in total heart content of sarcoplasmic, myofibrillar and stromal subcellular protein fractions. Analysis of *in vivo* synthesis, however, revealed that only myofibrillar protein synthesis was increased by rosiglitazone, indicating some degree of specificity of PPARγ agonism towards the contractile family of proteins. Rosiglitazone also tended to increase the percentage of myofibrillar protein renewed each day (fractional rate, +24%, $P = 0.07$), suggesting a concomitant increase in the turnover of these proteins. Because proteasome cannot degrade intact myofibrils [45], the calpains, a family of calcium-dependent proteases localized in the cardiac myofibrillar Z-disc that are under constant allosteric inhibition by calpastatin [46], were suggested to catalyze myofibrillar proteolysis, releasing disassembled peptides to the cytosol for ubiquitination and final proteolysis by the proteasome. In agreement with an increase in myofibrillar protein turnover, rosiglitazone treatment resulted in a significant reduction in cardiac calpastatin mRNA levels and protein content along with a marked increase in calpain activity, suggesting activation of calpain-mediated myofibrillar proteolysis. In contrast to calpains, but in agreement with a previous study in skeletal muscle [47], the β5 chymotryptic activity of the 26S proteasome was markedly reduced in rosiglitazone-treated rats along with the mRNA and protein levels of the 20S β5 proteasome subunits that was previously demonstrated to catalyze proteasome chymotryptic (cleavage of large hydrophobic groups) activity [48]. The mRNA levels of β2, which catalyzes proteasome tryptic (basic groups) activities, was also reduced by rosiglitazone [48]. In addition, rosiglitazone also decreased mRNA levels not only of the 19S RPN2 proteasome subunit, thought to participate in the recognition and binding of ubiquitin-like domains [48], but also of the ubiquitin ligases atrogin-1 and CHIP, which ubiquitinate and label proteins for proteasome-mediated proteolysis. The mechanisms by which rosiglitazone differentially modulates proteasome subunits are unknown, but clearly deserve further investigation. Due to its importance in quality control of the protein synthesis process [49], the marked reduction in 26S β5 (chymotryptic) proteasome activity found in rosiglitazone-treated rats, if not compensated by other proteolytic pathways, might result in accumulation of unfolded proteins, endoplasmic reticulum stress and worsening of cardiac function.

Investigation of signalling pathways that would explain the hypertrophic phenotype in rats under PPARγ agonist treatment revealed a marked activation of the mTOR pathway, as evidenced by increased levels of phosphorylated mTOR and its downstream substrates S6K1, S6, and 4E-BP1. By controlling the initiation of translation, which represents the limiting step in protein synthesis, mTOR can activate the assembly of the global ribosomal machinery and thus protein synthesis [50]. Of note is the fact that rosiglitazone-induced mTOR activation was not associated with concomitant activation of Akt, a well-known activator of the mTOR pathway, suggesting that mTOR activation was not linked to increased hormonal/growth-promoting signals such as insulin. These findings are in line with a recent study showing that PPARγ agonism was equally effective in producing cardiac hypertrophy in mice devoid of the insulin receptor (CIRKO) [8]. Alternatively to canonical insulin-mediated Akt stimulation, however, MAPK extracellular signal-regulated kinase (ERK), which is markedly activated in the heart by rosiglitazone, might be involved in the concomitant activation of the mTOR pathway. ERK was previously demonstrated to activate mTOR targets such as S6K1 and eIF4E in a process that involves phosphorylation and inactivation of tuberous sclerosis complex (TSC) 2, an

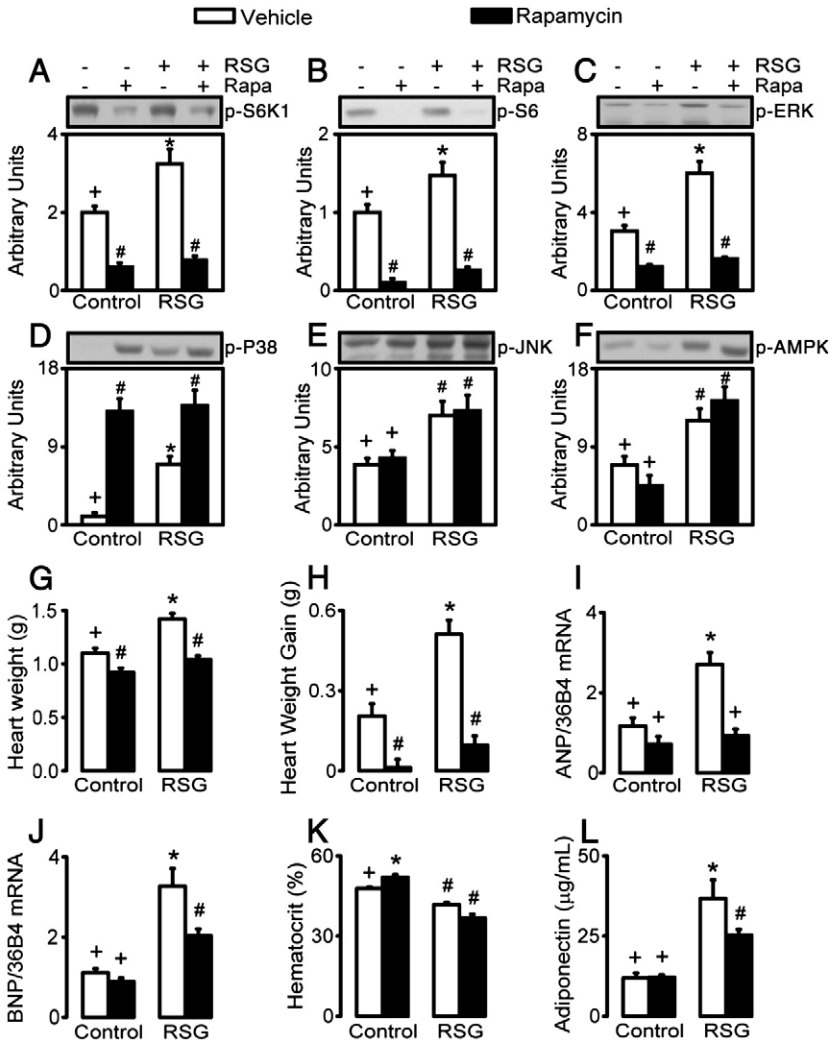

Fig. 5. Heart content of phospho (p)-S6K1 (panel A), p-S6 (panel B), p-ERK (panel C), p-P38 (panel D), p-JNK (panel E) and p-AMPK (panel F), final heart weight (panel G) and weight gain (final heart weight minus time zero heart weight, panel H), mRNA levels of ANP (panel I) and BNP (panel J), hematocrit (panel K) and plasma adiponectin concentration (panel L) in rats treated or not with rosiglitazone (RSG, 15 mg/kg day) and co-treated with daily injections of either vehicle or rapamycin (2 mg/kg day) for 15 days. $n = 6–8$ rats per group. Means not sharing a common superscript are significantly different from each other by two way ANOVA followed by Newman–Keuls' multiple range test, $P<0.05$.

inhibitor of mTOR activity [51,52]. Interestingly, rosiglitazone stimulation of ERK is dependent upon direct heart PPARγ activation [6], suggesting a role for the receptor in the activation of mTOR pathway and stimulation of protein synthesis.

Another germane finding of the present study is the dichotomic activation of both the mTOR pathway and AMPK in the heart of rosiglitazone-treated rats, in apparent contradiction with the role of AMPK as an inhibitor of mTOR through activation of TSC 1 and 2 [53,54]. It may be suggested, however, that AMPK activation might play a role in preventing excessive mTOR activation in cardiac muscle of rosiglitazone-treated animals. This could explain the elevated phosphorylation of eEF2 (hence reduced translational elongation) in the face of increased mTOR/S6K1 activation. Indeed, recent studies have shown that AMPK can inhibit eEF2-mediated translation despite mTOR/S6K1 activation in exercising/contracting skeletal muscles [55,56], suggesting that energy stress may override some hypertrophic translational signalling events.

Further supporting an important role of mTOR signalling in PPARγ-induced cardiac remodelling, pharmacological inhibition of mTOR with rapamycin completely blocked cardiac weight gain and increase in mRNA levels of the hypertrophic marker ANP induced by rosiglitazone. It is noteworthy that rapamycin blocked rosiglitazone-induced heart hypertrophy even in the presence of volume overload as evidenced by the reduced hematocrit percentage, and of elevated plasma adiponectin levels, indicating that the rapamycin effects were not related to indirect changes in some of the previously suggested underlying causes of the hypertrophy. In addition, among the three MAPKs previously demonstrated to be activated and considered as possible mediators of cardiac remodelling induced by rosiglitazone [6], rapamycin prevented heart hypertrophy even in the presence of either higher or unaltered phosphorylated contents of P38 and JNK, respectively. Only ERK had its activation by rosiglitazone blocked by rapamycin treatment. These data suggest that activation of both P38 and JNK, probably by volume overload and/or increased plasma adiponectin levels [6,57,58], does not result in heart hypertrophy in the absence of mTOR activation, further supporting an important role of this signalling pathway in the development of rosiglitazone-induced heart hypertrophy.

Whether activation of heart PPARγ has an inhibitory or a stimulatory role in the development of heart hypertrophy remains unresolved. Mice overexpressing PPARγ specifically in the heart display an eccentric cardiac hypertrophy with glycogen accumulation, heart dysfunction and increased ANP and BNP expression [9], very similar to the heart remodelling induced by TZDs reported here and earlier [4,6–8], which supports a direct positive role for heart PPARγ in the development of this type of hypertrophy. Considering that

eccentric and concentric (in which PPARγ activation results in attenuation of hypertrophy [5]) types of heart hypertrophy are mediated by completely different mechanisms and signalling pathways [57], it would not be surprising that PPARγ might have opposite roles in these conditions. In fact, the only similarity between the effects of TZDs in a normal heart presented here and the model of pressure-induced hypertrophy [5] is a reduction in cardiac wall thickness. Further studies are clearly needed to delineate the specific roles of cardiac PPARγ in these different types of heart remodelling.

In conclusion, this study presents strong evidence supporting the notion that, beyond elevated glycogen storage, rosiglitazone-induced cardiac hypertrophy is characterized by a particularly marked increase in myofibrillar protein synthesis associated with activation of the hypertrophic signalling pathway mTOR that, independently of the underlying cause, plays a fundamental role in the development of such cardiac remodelling. It will be of great interest to establish whether the signalling pathways identified herein also partake in PPARγ action in the human heart, which expresses much higher levels (8-fold) of the receptor compared to rodents [9].

Acknowledgments

The authors wish to gratefully acknowledge the invaluable technical assistance of Yves Gélinas, Sébastien Poulin, Pierre-Gilles Blanchard and Marie-Noëlle Cyr. This study was financially supported by grants from the Canadian Institutes of Health Research (CIHR) to YD and AM, Ph.D. Studentships from the Natural Sciences and Engineering Research Council of Canada and Fonds de la Recherche en Santé du Québec (FRSQ) to ML and VPH, and Postdoctoral Fellowships from a CIHR Training in Obesity Program grant to WTF and SB.

Appendix A. Supplementary data

Supplementary data associated with this article can be found, in the online version, at doi:10.1016/j.yjmcc.2009.04.011.

References

[1] Willson TM, Lambert MH, Kliewer SA. Peroxisome proliferator-activated receptor gamma and metabolic disease. Annu Rev Biochem 2001;70:341–67.
[2] Nissen SE, Wolski K. Effect of rosiglitazone on the risk of myocardial infarction and death from cardiovascular causes. N Engl J Med 2007;356(24):2457–71.
[3] Nesto RW, Bell D, Bonow RO, Fonseca V, Grundy SM, Horton ES, et al. Thiazolidinedione use, fluid retention, and congestive heart failure: a consensus statement from the American Heart Association and American Diabetes Association. October 7, 2003. Circulation 2003;108(23):2941–8.
[4] Yamamoto K, Ohki R, Lee RT, Ikeda U, Shimada K. Peroxisome proliferator-activated receptor gamma activators inhibit cardiac hypertrophy in cardiac myocytes. Circulation 2001;104(14):1670–5.
[5] Asakawa M, Takano H, Nagai T, Uozumi H, Hasegawa H, Kubota N, et al. Peroxisome proliferator-activated receptor gamma plays a critical role in inhibition of cardiac hypertrophy in vitro and in vivo. Circulation 2002;105(10):1240–6.
[6] Duan SZ, Ivashchenko CY, Russell MW, Milstone DS, Mortensen RM. Cardiomyocyte-specific knockout and agonist of peroxisome proliferator-activated receptor-gamma both induce cardiac hypertrophy in mice. Circ Res 2005;97(4):372–9.
[7] Edgley AJ, Thalen PG, Dahllof B, Lanne B, Ljung B, Oakes ND. PPARgamma agonist induced cardiac enlargement is associated with reduced fatty acid and increased glucose utilization in myocardium of Wistar rats. Eur J Pharmacol 2006;538(1–3):195–206.
[8] Sena S, Rasmussen IR, Wende AR, McQueen AP, Theobald HA, Wilde N, et al. Cardiac hypertrophy caused by peroxisome proliferator-activated receptor-gamma agonist treatment occurs independently of changes in myocardial insulin signaling. Endocrinology 2007;148(12):6047–53.
[9] Son NH, Park TS, Yamashita H, Yokoyama M, Huggins LA, Okajima K, et al. Cardiomyocyte expression of PPARgamma leads to cardiac dysfunction in mice. J Clin Invest 2007;117(10):2791–801.
[10] Sarbassov DD, Ali SM, Sabatini DM. Growing roles for the mTOR pathway. Curr Opin Cell Biol 2005;17(6):596–603.
[11] Gao XM, Wong G, Wang B, Kiriazis H, Moore XL, Su YD, et al. Inhibition of mTOR reduces chronic pressure-overload cardiac hypertrophy and fibrosis. J Hypertens 2006;24(8):1663–70.
[12] Kuzman JA, O'Connell TD, Gerdes AM. Rapamycin prevents thyroid hormone-induced cardiac hypertrophy. Endocrinology 2007;148(7):3477–84.
[13] Kemi OJ, Ceci M, Wisloff U, Grimaldi S, Gallo P, Smith GL, et al. Activation or inactivation of cardiac Akt/mTOR signaling diverges physiological from pathological hypertrophy. J Cell Physiol 2008;214(2):316–21.
[14] Depre C, Wang Q, Yan L, Hedhli N, Peter P, Chen L, et al. Activation of the cardiac proteasome during pressure overload promotes ventricular hypertrophy. Circulation 2006;114(17):1821–8.
[15] Letavernier E, Perez J, Bellocq A, Mesnard L, de Castro Keller A, Haymann JP, et al. Targeting the calpain/calpastatin system as a new strategy to prevent cardiovascular remodeling in angiotensin II-induced hypertension. Circ Res 2008;102(6):720–8.
[16] Lane RD, Mellgren RL, Mericle MT. Subcellular localization of bovine heart calcium-dependent protease inhibitor. J Mol Cell Cardiol 1985;17(9):863–72.
[17] Yang X, Smith U. Adipose tissue distribution and risk of metabolic disease: does thiazolidinedione-induced adipose tissue redistribution provide a clue to the answer? Diabetologia 2007;50(6):1127–39.
[18] Maeda K, Shioi T, Kosugi R, Yoshida Y, Takahashi K, Machida Y, et al. Rapamycin ameliorates experimental autoimmune myocarditis. Int Heart J 2005;46(3):513–30.
[19] Shioi T, McMullen JR, Tarnavski O, Converso K, Sherwood MC, Manning WJ, et al. Rapamycin attenuates load-induced cardiac hypertrophy in mice. Circulation 2003;107(12):1664–70.
[20] Belcher EH, Harriss EB. Studies of plasma volume, red cell volume and total blood volume in young growing rats. J Physiol 1957;139(1):64–78.
[21] Lo S, Russell JC, Taylor AW. Determination of glycogen in small tissue samples. J Appl Physiol 1970;28(2):234–6.
[22] Folch J, Lees M, Sloane Stanley GH. A simple method for the isolation and purification of total lipides from animal tissues. J Biol Chem 1957;226(1):497–509.
[23] Bass A, Brdiczka D, Eyer P, Hofer S, Pette D. Metabolic differentiation of distinct muscle types at the level of enzymatic organization. Eur J Biochem 1969;10(2):198–206.
[24] Sokoloff L, Reivich M, Kennedy C, Des Rosiers MH, Patlak CS, Pettigrew KD, et al. The [^{14}C]deoxyglucose method for the measurement of local cerebral glucose utilization: theory, procedure, and normal values in the conscious and anesthetized albino rat. J Neurochem 1977;28(5):897–916.
[25] Ferre P, Leturque A, Burnol AF, Penicaud L, Girard J. A method to quantify glucose utilization in vivo in skeletal muscle and white adipose tissue of the anaesthetized rat. Biochem J 1985;228(1):103–10.
[26] Somogyi M. Determination of blood sugar. J Biol Chem 1945;160:69–73.
[27] Festuccia WT, Oztezcan S, Laplante M, Berthiaume M, Michel C, Dohgu S, et al. Peroxisome proliferator-activated receptor-g-mediated positive energy balance in the rat is associated with reduced sympathetic drive to adipose tissues and thyroid status. Endocrinology 2008;149(5):2121–30.
[28] Garlick PJ, McNurlan MA, Preedy VR. A rapid and convenient technique for measuring the rate of protein synthesis in tissues by injection of [^{3}H] phenylalanine. Biochem J 1980;192(2):719–23.
[29] Hunter RJ, Patel VB, Miell JP, Wong HJ, Marway JS, Richardson PJ, et al. Diarrhea reduces the rates of cardiac protein synthesis in myofibrillar protein fractions in rats in vivo. J Nutr 2001;131(5):1513–9.
[30] Dahlmann B, Kuehn L, Rutschmann M, Reinauer H. Purification and characterization of a multicatalytic high-molecular-mass proteinase from rat skeletal muscle. Biochem J 1985;228(1):161–70.
[31] Sawada H, Muto K, Fujimuro M, Akaishi T, Sawada MT, Yokosawa H, et al. Different ratios in 20 S proteasomes and regulatory subunit complexes in two isoforms of the 26 S proteasome purified from rabbit skeletal muscle. FEBS Lett 1993;335(2):207–12.
[32] Tanaka K, Ii K, Ichihara A, Waxman L, Goldberg AL. A high molecular weight protease in the cytosol of rat liver. I. Purification, enzymological properties, and tissue distribution. J Biol Chem 1986;261(32):15197–203.
[33] Powell SR, Davies KJ, Divald A. Optimal determination of heart tissue 26S-proteasome activity requires maximal stimulating ATP concentrations. J Mol Cell Cardiol 2007 Jan;42(1):265–9.
[34] Plante E, Lachance D, Gaudreau M, Drolet MC, Roussel E, Arsenault M, et al. Effectiveness of beta-blockade in experimental chronic aortic regurgitation. Circulation 2004;110(11):1477–83.
[35] Quinones MA, Waggoner AD, Reduto LA, Nelson JG, Young JB, Winters Jr WL, et al. A new, simplified and accurate method for determining ejection fraction with two-dimensional echocardiography. Circulation 1981;64(4):744–53.
[36] Tei C, Ling LH, Hodge DO, Bailey KR, Oh JK, Rodeheffer RJ, et al. New index of combined systolic and diastolic myocardial performance: a simple and reproducible measure of cardiac function—a study in normals and dilated cardiomyopathy. J Cardiol 1995;26(6):357–66.
[37] Slama M, Ahn J, Peltier M, Maizel J, Chemla D, Varagic J, et al. Validation of echocardiographic and Doppler indexes of left ventricular relaxation in adult hypertensive and normotensive rats. Am J Physiol Heart Circ Physiol 2005;289(3):H1131–6.
[38] Brodie BB, Costa E, Dlabac A, Neff NH, Smookler HH. Application of steady state kinetics to the estimation of synthesis rate and turnover time of tissue catecholamines. J Pharmacol Exp Ther 1966;154(3):493–8.
[39] Luptak I, Shen M, He H, Hirshman MF, Musi N, Goodyear LJ, et al. Aberrant activation of AMP-activated protein kinase remodels metabolic network in favor of cardiac glycogen storage. J Clin Invest 2007;117(5):1432–9.
[40] Ahuja P, Sdek P, MacLellan WR. Cardiac myocyte cell cycle control in development, disease, and regeneration. Physiol Rev 2007;87(2):521–44.
[41] Arad M, Maron BJ, Gorham JM, Johnson Jr WH, Saul JP, Perez-Atayde AR, et al. Glycogen storage diseases presenting as hypertrophic cardiomyopathy. N Engl J Med 2005;352(4):362–72.

[42] Golfman LS, Wilson CR, Sharma S, Burgmaier M, Young ME, Guthrie PH, et al. Activation of PPARgamma enhances myocardial glucose oxidation and improves contractile function in isolated working hearts of ZDF rats. Am J Physiol Endocrinol Metab 2005;289(2):E328–36.
[43] Buhl ES, Jessen N, Schmitz O, Pedersen SB, Pedersen O, Holman GD, et al. Chronic treatment with 5-aminoimidazole-4-carboxamide-1-beta-D-ribofuranoside increases insulin-stimulated glucose uptake and GLUT4 translocation in rat skeletal muscles in a fiber type-specific manner. Diabetes 2001;50(1):12–7.
[44] Taha M, Lopaschuk GD. Alterations in energy metabolism in cardiomyopathies. Ann Med 2007;39(8):594–607.
[45] Solomon V, Goldberg AL. Importance of the ATP–ubiquitin–proteasome pathway in the degradation of soluble and myofibrillar proteins in rabbit muscle extracts. J Biol Chem 1996;271(43):26690–7.
[46] Goll DE, Thompson VF, Li H, Wei W, Cong J. The calpain system. Physiol Rev 2003;83(3):731–801.
[47] Wang X, Hu Z, Hu J, Du J, Mitch WE. Insulin resistance accelerates muscle protein degradation: activation of the ubiquitin–proteasome pathway by defects in muscle cell signaling. Endocrinology 2006;147(9):4160–8.
[48] Powell SR. The ubiquitin–proteasome system in cardiac physiology and pathology. Am J Physiol Heart Circ Physiol 2006;291(1):H1–H19.
[49] Dickhout JG, Austin RC. Proteasomal regulation of cardiac hypertrophy: is demolition necessary for building? Circulation 2006;114(17):1796–8.
[50] Hedhli N, Pelat M, Depre C. Protein turnover in cardiac cell growth and survival. Cardiovasc Res 2005;68(2):186–96.
[51] Ma L, Chen Z, Erdjument-Bromage H, Tempst P, Pandolfi PP. Phosphorylation and functional inactivation of TSC2 by Erk implications for tuberous sclerosis and cancer pathogenesis. Cell 2005;121(2):179–93.
[52] Rolfe M, McLeod LE, Pratt PF, Proud CG. Activation of protein synthesis in cardiomyocytes by the hypertrophic agent phenylephrine requires the activation of ERK and involves phosphorylation of tuberous sclerosis complex 2 (TSC2). Biochem J 2005;388(Pt 3):973–84.
[53] Inoki K, Li Y, Zhu T, Wu J, Guan KL. TSC2 is phosphorylated and inhibited by Akt and suppresses mTOR signalling. Nat Cell Biol 2002;4(9):648–57.
[54] Han S, Zheng Y, Roman J. Rosiglitazone, an agonist of PPARgamma, inhibits non-small cell carcinoma cell proliferation in part through activation of tumor sclerosis complex-2. PPAR Res 2007:29632.
[55] Dreyer HC, Fujita S, Cadenas JG, Chinkes DL, Volpi E, Rasmussen BB. Resistance exercise increases AMPK activity and reduces 4E-BP1 phosphorylation and protein synthesis in human skeletal muscle. J Physiol 2006;576(Pt 2):613–24.
[56] Thomson DM, Fick CA, Gordon SE. AMPK activation attenuates S6K1, 4E-BP1, and eEF2 signaling responses to high-frequency electrically stimulated skeletal muscle contractions. J Appl Physiol 2008;104(3):625–32.
[57] Sopontammarak S, Aliharoob A, Ocampo C, Arcilla RA, Gupta MP, Gupta M. Mitogen-activated protein kinases (p38 and c-Jun NH2-terminal kinase) are differentially regulated during cardiac volume and pressure overload hypertrophy. Cell Biochem Biophys 2005;43(1):61–76.
[58] Shibata R, Ouchi N, Ito M, Kihara S, Shiojima I, Pimentel DR, et al. Adiponectin-mediated modulation of hypertrophic signals in the heart. Nat Med 2004;10(12):1384–9.